

COMMISSIONS 27 AND 42 OF THE IAU  
INFORMATION BULLETIN ON VARIABLE STARS

Number 6003

Konkoly Observatory  
Budapest  
11 November 2011  
*HU ISSN 0374 – 0676*

**IMPLICATIONS OF THE NON-DETECTION OF X-RAY EMISSION  
FROM HD 149427**

STUTE, M.<sup>1</sup>; LUNA, G.J.M.<sup>2,3</sup>

<sup>1</sup> Institute for Astronomy and Astrophysics, Section Computational Physics, Eberhard Karls University Tübingen, Auf der Morgenstelle 10, 72076 Tübingen, Germany

<sup>2</sup> Instituto de Ciencias Astronomicas, de la Tierra y del Espacio (ICATE), Av.Espana Sur 1512, J5402DSP, San Juan, Argentina

<sup>3</sup> Harvard-Smithsonian Center for Astrophysics, 60 Garden St. MS 15, Cambridge, MA, 02138, USA

HD 149427 (PC 11 = IRAS 16336-5536 = PN G 331.1-05.7) was first noticed to be a peculiar object by Webster (1966). Its exact nature is not known, several scenarios exist in the literature.

The object is listed in the Planetary Nebula (PN) catalogue of Peimbert & Costero (1961) as PC 11, in the catalogue of Southern PNe of Henize (1967) as Hen 2-172 and in the catalogue of Henize (1976) as Hen 3-1223 based on its H $\alpha$  emission. Henize (1976) noted that the emission-line spectrum is that of a PN but with a continuum of an F star. Gutierrez-Moreno et al. (1987) systematically investigated HD 149427 using optical photographic, spectro- photometric and spectroscopic observations. They suggested that it is indeed a young peculiar PN. Gutierrez-Moreno et al. (1995) confirmed this with a diagram using the ratios of [OIII] $\lambda$ 4363/H $\gamma$  and [OIII] $\lambda$ 5007/H $\beta$ . Parthasarathy et al. (2000) suggested that the central star is a close binary system with an early-F dwarf companion based on UV variations. Webster (1966) classified the object as a Symbiotic Star (SyS) based on its spectrum. Using NIR observations, Glass & Webster (1973) classified HD 149427 as SyS with a yellow supergiant as cool component, however, their NIR observations could not reliably identify its nature. Allen & Glass (1974) confirmed this result with new NIR observation, but pointed out the high density and high excitation in the nebulosity. Allen (1982) listed it as a D'-type SyS.

The distance is also very uncertain. Milne & Aller (1975) detected 5 GHz radio emission and estimated the distance  $> 6.7$  kpc based on its radio flux. Milne (1979) revised the 5 GHz catalogue of PNe and listed a radio distance of  $> 10.5$  kpc. However, it has been shown that a nearby radio source may be confused with HD 149427 (Wright & Allen 1978). Maciel (1984) used a relationship between nebular ionized mass and radius and estimated a distance of  $< 6.2$  kpc. Gutierrez-Moreno et al. (1987) estimated a distance of about 3 kpc. Kenny (1995) used radio observations for determining the distance of about 5 kpc. Gutierrez-Moreno & Moreno (1998) measured the spectral type of the late component of the central star and, using NIR colors of Glass & Webster (1973), determined a small distance of 420 pc assuming a luminosity class V. Assuming that the cool component is, however, a giant of luminosity class III, this estimated distance had to be increased to

850 pc (Gutierrez-Moreno & Moreno 1998). Tajitsu & Tamura (1998) derived a distance of 9 kpc using IRAS four-band fluxes. Phillips (2001) used the observed radial velocities of PNe and the galactic rotation curve for measuring the distance to 3.27 kpc. Pereira et al. (2010) analyzed high resolution spectra of the late-type companion and found  $\log g$  and  $T$  values implying a distance of 9.94 kpc. However, using the luminosity of the white dwarf in the system, the distance of about 10 kpc would result in a extremely large white dwarf radius of  $0.14 R_{\odot}$  (Pereira et al. 2010).

HD 149427 received our attention since it is a member of the list of symbiotic stars with possible jet detections compiled by Brocksopp et al. (2004). Brocksopp et al. (2003) found three peaks and extended emission in HST WFPC2 snapshot images taken in July 1999 with F502N and F656N filters corresponding to the central source and knots at distances of about  $2''$  and  $12''$ . Radio observations show extended emission in the same direction as the peaks in the HST images (Brocksopp et al. 2003). Gutierrez-Moreno & Moreno (1998) found evidence for jet-like [OIII] emission moving away from the central nebula with a velocity of  $120 \text{ km s}^{-1}$ .

X-ray observations provide a direct probe of the two most important components of jet-driving systems: the bow and internal shocks of the jet emitting soft X-rays and the central parts of the jet engine, where gas is being accreted to power the jet, leading to hard X-ray emission. Currently R Aqr (Kellogg et al. 2001, 2007) and CH Cyg (Galloway & Sokoloski 2004; Karovska et al. 2007, 2010) are the only two jets from symbiotic stars that have been resolved in X-rays. All objects with jets, detected in other wavelength, when observed in X-rays, show soft components ( $< 2 \text{ keV}$ ; R Aqr, CH Cyg, MWC 560, RS Oph, AG Dra, Z And, V1329 Cyg). The three objects CH Cyg, R Aqr, MWC 560 also emit hard components (Mukai et al. 2007; Nichols et al. 2007; Stute & Sahai 2009). Z And showed hard emission in one of three observations only (Sokoloski et al. 2006).

The paper is organized as follows: in Section 1, we show details of the observations and the analysis of the data. After that we describe the results in Section 2. We end with a discussion and conclusions in Sections 3 and 4.

## 1 Observation and analysis

We observed the field of HD 149427 with *XMM-Newton* in 2009 (Table 1) using the EPIC instrument operated in full window mode and with the medium thickness filter. Simultaneously, we used the Optical Monitor OM. All the data reduction was performed using the Science Analysis Software (SAS) software package<sup>1</sup> version 8.0. We removed events at periods with high background levels from the pipeline products selecting events with pattern 0–4 (only single and double events) for the pn and pattern 0–12 for the MOS, respectively, and applying the filter FLAG=0. The resulting exposure time after these steps is 33.5 ks.

## 2 Results

### 2.1 Images

All three X-ray images with the EPIC pn, MOS1 and MOS2 cameras show no detection of emission above background levels centered on HD 149427 using the coordinates from SIMBAD (Fig. 1, white circles). In all bands, however, a faint source is visible which

---

<sup>1</sup><http://xmm.vilspa.esa.es/>

Table 1: Observations on September 01/02, 2009 (ObsID: 0604920201)

Instrument	Filter	Duration	UT Start	UT Stop
pn	Medium	68430	19:05:32	14:06:02
MOS1	Medium	69504	18:43:12	14:01:36
MOS2	Medium	69515	18:43:11	14:01:46
OM	U	10× ~1500	18:51:36	23:49:51
	UVW1	10× ~1500	00:40:11	06:08:27
	UVM2	15× ~1500	06:13:48	15:02:12

is about 26" away from the nominal position of HD 149427. According to Kerber et al. (2008), the proper motion of HD 149427 is of the order of a few mas in RA and about 20 mas in Dec, thus too small for explaining this discrepancy. In order to check, whether possible pointing errors arose during our XMM observations, we created images in the soft and hard band for all three cameras, ran a source detection with EDETECT and finally identified the closest 11 objects listed by SIMBAD in our mosaic. Fig. 2 shows the mosaic including our detected X-ray sources (white circles), the reference objects from SIMBAD (green circles) and also the closest source from the ROSAT faint source all-sky survey (red circle). While the pointing uncertainties in the ROSAT mission are obvious, we can clearly identify three objects, for which the SIMBAD position agrees perfectly with the position found in our source detection run (white arrows). Therefore we can exclude any pointing error and indeed report the non-detection of HD 149427 in X-rays.

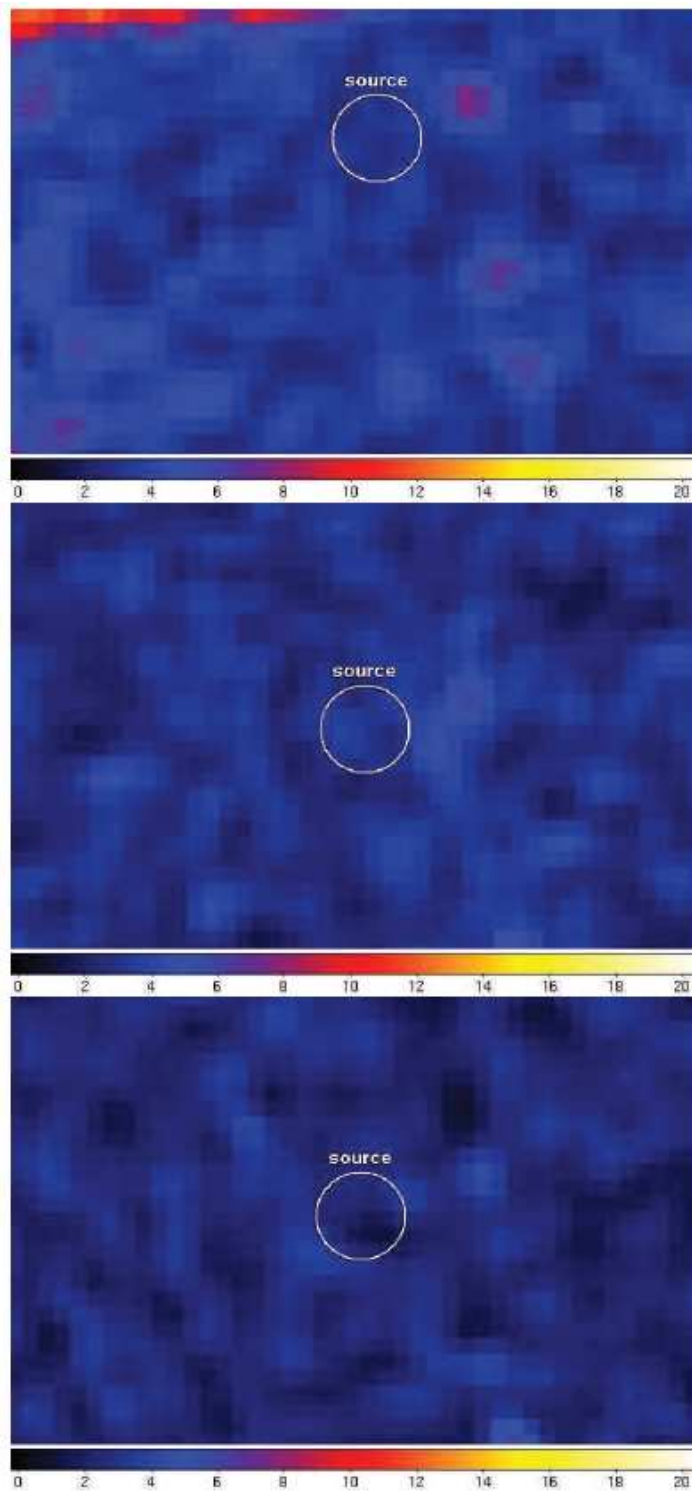
Contrary to the X-ray band, HD 149427 has been detected in the three optical bands used. The average magnitudes in the optical filters U, UVW1 and UVM2 are 12.7, 13.5 and 14.8, respectively. The slope of the spectral energy distribution indicates that the optical flux is dominated by nebular emission (Fig. 3). The flux levels of blackbody emission corresponding to a white dwarf with a radius of  $8 \times 10^8$  cm and with an effective temperature of 105000 K at a distance of 850 pc (Gutierrez-Moreno & Moreno 1998) are lower than the measured fluxes.

## 2.2 Light curves

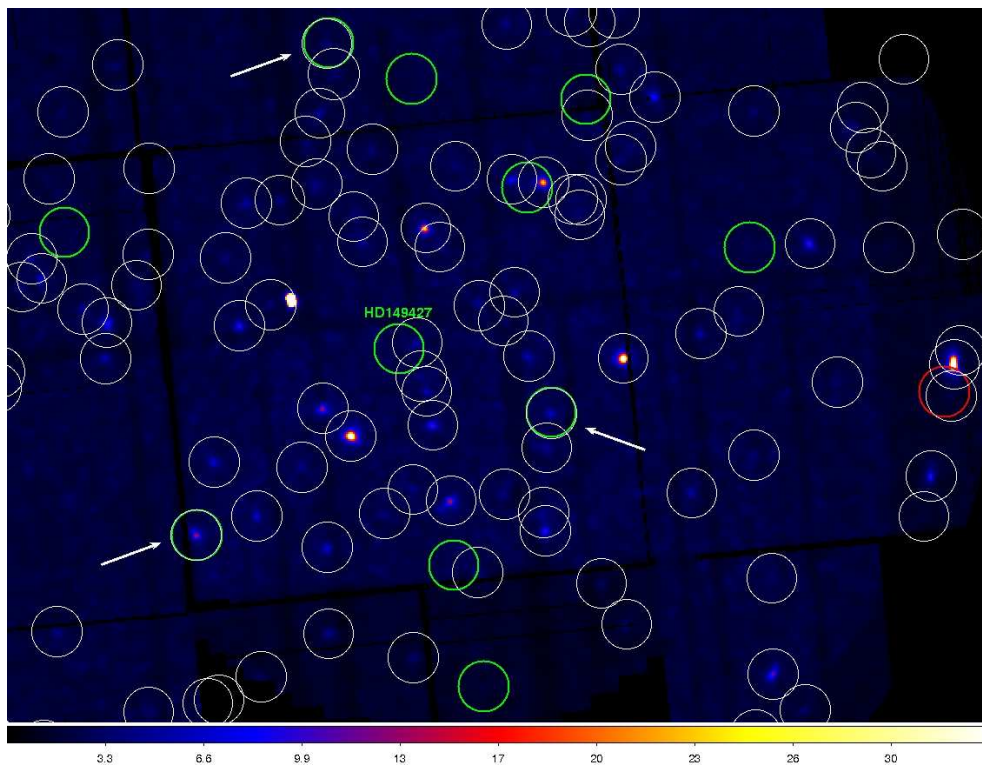
We examined the OM photometry (Fig. 4). The optical light curves are consistent with a constant flux. The measured rms variations, those expected from Poisson statistics, and the ratios of these two quantities are listed in Table 2.  $s$  and  $s_{exp}$  are given in percentage of the mean value. The optical light curves in filters UVW1 and UVM2 where the ratio of measured to expected rms  $s/s_{exp}$  is 1.27 and 1.21, respectively, may indicate weak variability, however, the presence of systematic and/or unknown errors is more likely. Since the optical flux is dominated by nebular emission, we do not expect variability in these bands.

Table 2: Measured and expected variations and their ratio

optical filter	measured variation $s$	expected variation $s_{exp}$	ratio $s/s_{exp}$
U	0.044 %	0.045 %	0.96
UVW1	0.045 %	0.046 %	1.27
UVM2	0.288 %	0.237 %	1.21



**Figure 1.** EPIC images of the region around HD 149427; top: pn, middle: MOS1, bottom: MOS2; colors show the number of counts.



**Figure 2.** Mosaic of EPIC images of the region around HD 149427 including our detected X-ray sources (white circles), the reference objects from SIMBAD (green circles) and also the closest source from the ROSAT faint source all-sky survey (red circle). We can clearly identify three objects, for which the SIMBAD position agrees perfectly with the position found in our source detection run (white arrows) and thus can exclude any pointing error and indeed report the non-detection of HD 149427 in X-rays.

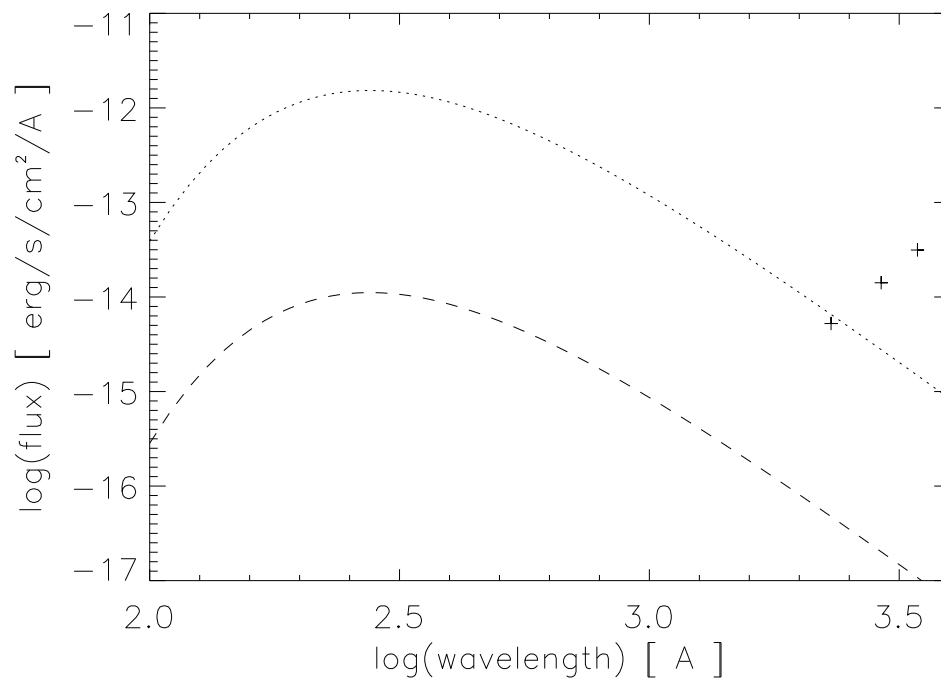


**Figure 3.** Spectral energy distribution in the optical filters U, UVW1 and UVM2. Also plotted is blackbody emission representing a white dwarf with a temperature of 105000 K and radius of  $8 \times 10^8$  cm at distances of 850 pc (dotted line) and 9.96 kpc (dashed line). The slope and flux level of the spectral energy distribution indicate that the optical flux is dominated by nebular emission.

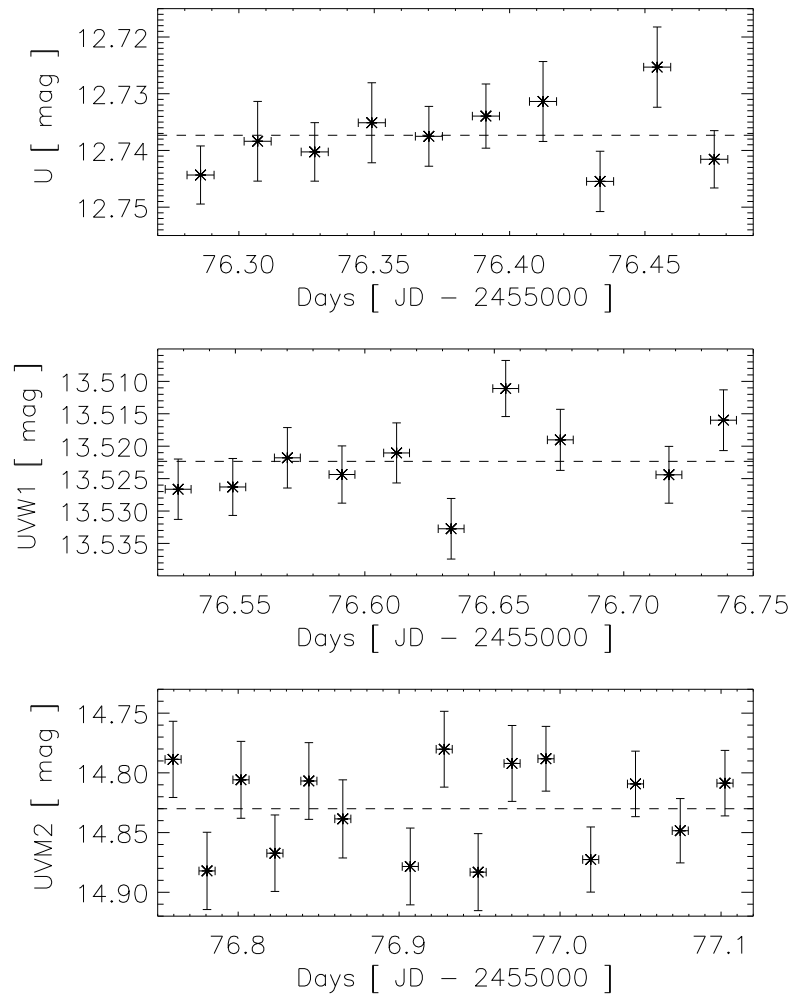


**Figure 4.** Light curves of the OM exposures for filters U (top, 3440 Å), UVW1 (middle, 2910 Å) and UVM2 (bottom, 2310 Å). The dotted lines show the average magnitude.

### 3 Discussion

We reported the non-detection of X-rays from the jet-driving symbiotic star HD 149427 using *XMM-Newton*. However, we detected HD 149427 with the Optical Monitor and extracted light curves in the filters U (3440 Å), UVW1 (2910 Å) and UVM2 (2310 Å). The light curves in filters UVW1 and UVM2 show hints for variability, however, due to possible systematic and/or unknown errors, they are also consistent with a constant flux. The UV spectral energy distribution indicate that the optical flux is dominated by nebular emission.

Using the effective exposure time of 33.5 ks in all instruments, the sensitivity of *XMM-Newton* (Watson et al. 2001) gives an upper limit of about  $10^{-15}$  erg s $^{-1}$  cm $^{-2}$  in the soft band ( $< 2$  keV) and of about  $10^{-14}$  erg s $^{-1}$  cm $^{-2}$  in the hard band ( $> 2$  keV).

#### 3.1 What is the nature of HD 149427?

We can identify several different scenarios for the nature of HD 149427 in the literature: a planetary nebula or a symbiotic star, both either close to us or very distant.

Pereira et al. (2010) favor the idea of HD 149427 being a distant PN at about 10 kpc away from us. From the position of HD 149427 in the [OIII] $\lambda$ 5007/H $\beta$  – [OIII] $\lambda$ 4363/H $\gamma$  diagram, they claim it is neither consistent with that of PNe nor that of symbiotic stars. They argue that the electron density observed in HD 149427 is higher than typical electron densities in PNe, but not as high as observed in D- and D'-type symbiotics. However, the closest object to HD 149427 in this diagram is another D'-type symbiotic. Or is HD 149427 a symbiotic star whose companion just turns into a PN?

In case of HD 149427 being a central star of a PN, we simply expect X-ray emission from a blackbody with a temperature of about  $10^5$  K (Gutierrez-Moreno & Moreno 1998) as given in Fig. 3. The emission at 0.2 keV (= 62 Å) would be fainter than our upper limits, so our non-detection would have no significant implications.

However, if HD 149427 was a symbiotic star and accretion was present in this object, we would be able to test the accretion rate with important implications (see below).

#### 3.2 What is the distance to HD 149427?

For deriving the distance to HD 149427, Pereira et al. (2010) used their fits to high resolution spectra, namely their derived values of  $\log g$  and  $\log T$ . They estimated the luminosity of the star and calculated the distance to it using a measured  $V$  magnitude. They finally derived a distance of  $9.94 \pm 0.6$  kpc. However, using the luminosity of the white dwarf in the system, the distance would result in a extremely large white dwarf radius of  $0.14 R_{\odot}$  (Pereira et al. 2010). Turning this argument around and using radius determinations of  $0.01$ – $0.02 R_{\odot}$  (e.g. Gutierrez-Moreno & Moreno 1998), we would get a distance of about  $0.7$ – $1.5$  kpc. A second point of criticism is that the error estimate mentioned above bases only on the error of  $\log g$  and  $\log T$ , but not on the error of the  $V$  magnitude. The  $V$  magnitudes in the literature vary between 11.2 and 12.7 – the latter value has been used by Pereira et al. (2010). The former value, however, would imply a distance of only about 5 kpc, thus the distance based only on their own data is still highly uncertain. The smallest estimated distance to HD 149427 is only 850 pc (Gutierrez-Moreno & Moreno 1998), therefore we adopt two extremal distances of 850 pc and 10 kpc.

With a distance of 850 pc, the flux upper limits give an upper limit for the soft X-ray luminosity of about  $8.6 \times 10^{28}$  erg s $^{-1}$  and for the hard X-ray luminosity of about  $8.6 \times 10^{29}$

erg s<sup>-1</sup>; with the highest claimed distance of 9.96 kpc, these limits increase to  $1.2 \times 10^{31}$  erg s<sup>-1</sup> and  $1.2 \times 10^{32}$  erg s<sup>-1</sup>, respectively.

### 3.3 Implications for the accretion process

Since accretion should be the main source of hard X-ray emission in this objects, we can convert these upper limits of luminosities into upper limits for the accretion rates. From the definition

$$L_{\text{acc}} \lesssim \frac{1}{2} \frac{GM\dot{M}}{R} = 3 \times 10^{32} \text{ erg s}^{-1} \left( \frac{M}{0.6 M_{\odot}} \right) \left( \frac{\dot{M}}{10^{-10} M_{\odot} \text{ yr}^{-1}} \right) \left( \frac{8 \times 10^8 \text{ cm}}{R} \right) \quad (1)$$

follows that, after assuming the largest distance, the white dwarf accretes with a rate below  $10^{-10} M_{\odot} \text{ yr}^{-1}$ . At these low accretion rates, a boundary layer between the accretion disk and the surface of the white dwarf is optically thin (Pringle & Savonije 1979; Popham & Narayan 1995) and thus emitting hard X-rays with  $L_{\text{acc}}$ . In case, the low distance of 850 pc is correct, the upper limit on the accretion rate reduces even to  $10^{-13} M_{\odot} \text{ yr}^{-1}$ .

### 3.4 Implications for the jet

Gutierrez-Moreno & Moreno (1998) found an electron density of the potential jet knot of  $10^5 \text{ cm}^{-3}$ , an electron temperature of 20000 K and a velocity of this knot of 120 km s<sup>-1</sup>. With a typical ionization fraction at this temperature and a typical compression factor – we assume that the observed values correspond to those of shocked jet material – we derive an (un-shocked) jet density in the same order of magnitude as the measured electron density.

The jet velocity is connected to the velocity of the contact discontinuity or knot via

$$v_{\text{knot}} = v_{\text{jet}} \frac{\sqrt{\eta}}{1 + \sqrt{\eta}} \quad (2)$$

with  $\eta$  being the ratio of jet to ambient density. Therefore the jet velocity is always higher than the knot propagation velocity (e.g. a factor 4.2 for  $\eta = 0.1$  or 1.3 for  $\eta = 10$ ). The presence of a jet with a velocity of about 120 km s<sup>-1</sup> naturally leads to shocks with temperatures of the order of 0.02 keV, which contribute only marginally to the bands observed with *XMM-Newton* or *Chandra*. Higher velocities above 300 km s<sup>-1</sup>, however, should lead to soft X-ray emission. Assuming a cylindrical jet with a radius of about 1 AU, the mass-loss rate in the jet is

$$\dot{M}_{\text{jet}} = \pi R_{\text{jet}}^2 n_{\text{jet}} m_{\text{H}} v_{\text{jet}} > 2.3 \times 10^{-11} M_{\odot} \text{ yr}^{-1}. \quad (3)$$

Since the mass-loss rate through the jet is at most a few percent of the mass accretion rate (depending on the underlying jet formation model), the latter must have been of the order of  $10^{-10} - 10^{-8} M_{\odot} \text{ yr}^{-1}$  at the time when the jet was formed.

The kinetic luminosity of the jet would be

$$L_{\text{kin}} = \frac{1}{2} \dot{M}_{\text{jet}} v_{\text{jet}}^2 > 2 \times 10^{29} \text{ erg s}^{-1}. \quad (4)$$

Only a fraction of this kinetic luminosity ( $\sim 1-20$  %, Stute & Sahai 2007) would be radiated away in soft X-rays, thus the presence of an X-ray emitting jet cannot be ruled out

by our non-detection, independent of adopting the small or large distance. Furthermore we can argue that if a larger fraction of the proposed observation time had not been affected by high background, we might have detected soft emission from the jet.

Another source of soft X-ray emission might be the presence of colliding winds as in  $\beta$  systems classified by Mürset et al. (1991) and Mürset et al. (1997). Their typical luminosity may also be of the order of  $10^{31}$  erg s<sup>-1</sup>.

## 4 Conclusion

We reported the non-detection of X-ray emission from the enigmatic object HD 149427. This result poses upper limits on the mass accretion rate of the white dwarf. Such low accretion rates are untypical for symbiotic stars and may favor the picture of HD 149427 being a young PN, even if we adopt the larger values of its distance. Unfortunately, the distance to HD 149427 is still highly uncertain.

We estimated the possible mass-loss rate and kinetic luminosity of the jet and found no contradiction with our upper limit of soft X-ray emission. If a larger fraction of the proposed observation time had not been affected by high background, we might have detected soft emission from the jet. Therefore new X-ray observations might give new exciting results for this enigmatic object.

ACKNOWLEDGMENTS: This work is based on observations obtained with *XMM-Newton*, an ESA science mission with instruments and contributions directly funded by ESA Member States and the USA (NASA). GJML thanks NASA for funding this work by XMM-Newton AO-8 award NNX09AP88G.

### References:

- Allen, D.A., Glass, I.S. 1974, MNRAS, 167, 337  
 Allen, D.A. 1982, in: IAU Colloquium 70 on “The Nature of Symbiotic stars”, p. 225, Friedjung M., Viotti R. (eds.), Reidel  
 Brocksopp, C., Bode, M. F., Eyres, S. P. S. 2003, MNRAS, 344, 1264  
 Brocksopp, C., Sokoloski, J. L., Kaiser, C., et al. 2004, MNRAS, 347, 430  
 Galloway, D. K., Sokoloski, J. L. 2004, ApJ, 613, L61  
 Glass, I.S., Webster, B.L. 1973, MNRAS, 165, 77  
 Gutierrez-Moreno, A., Moreno, H. 1998, PASP, 110, 458  
 Gutierrez-Moreno, A., Moreno, H., Cortes, G. 1987, Rev. Mex. A. A., 14, 344  
 Gutierrez-Moreno, A., Moreno, H., Cortes, G. 1995, PASP, 107, 462  
 Henize, K.G. 1967, ApJS, 14, 125  
 Henize, K.G. 1976, ApJS, 30, 491  
 Karovska, M., Carilli, C. L., Raymond, J. C., Mattei, J. A. 2007, ApJ, 661, 1048  
 Karovska, M., Gaetz, T. J., Carilli, C. L., Hack, W., Raymond, J. C., Lee, N. P. 2010, ApJ, 710, 132  
 Kellogg, E., Pedelty, J. A., Lyon, R. G. 2001, ApJ, 563, 151  
 Kellogg, E., Anderson, C., Korreck, K, et al. 2007, ApJ, 664, 1079  
 Kenny, H.T. 1995, PhD Thesis, University of Calgary  
 Kerber, F., Mignani, R. P., Smart, R. L., Wicenc, A. 2008, A & A, 479, 155  
 Maciel, W. J. 1984, A & AS, 55, 253

- Milne, D.K. 1979, A & AS, 36, 227  
Milne, D.K., Aller, L.H. 1975, A & A, 38, 183  
Mukai, K., Ishida, M., Kilbourne, C., et al. 2006, PASJ, 59, 177  
Mürset, U., Nussbaumer, H., Schmid, H. M., Vogel, M. 1991, A & A 248, 458  
Mürset, U., Wolff, B., Jordan, S. 1997, A & A 319, 201  
Nichols, J. S., DePasquale, J., Kellogg, E., et al. 2007, ApJ, 660, 651  
Parthasarathy, M., Garcia-Lario, P., Pottasch, S. R., et al. 2000, A & A, 355, 720  
Peimbert, M., Costero, R. 1961, BOTT, 3, 33  
Pereira, C. B., Baella, N. O., Daflon, S., Miranda, L. F. 2010, A & A, 509, A13  
Phillips, J.P. 2001, A & A, 367, 967  
Popham, R., Narayan, R. 1995, ApJ, 442, 337  
Pringle, J. E., Savonije, G. J. 1979, MNRAS, 187, 777  
Sokoloski, J. L., Kenyon, S. J., Espey, B. R., et al. 2006, ApJ, 636, 1002  
Stute, M., Sahai, R. 2007, ApJ, 665, 698  
Stute, M., Sahai, R. 2009, A & A, 498, 209  
Tajitsu, A., Tamura, S. 1998, AJ, 115, 1989  
Watson, M. G., Augueres, J.-L., Ballet, J., et al. 2001, A & A, 365, L51  
Webster, L. B. 1966, PASP, 78, 136  
Wright, A.E., Allen, D.A. 1978, MNRAS, 184, 893